



Title	Free-Standing Nanometer-Thick Covalent Organic Framework Films for Separating CO <sub>2</sub> and N <sub>2</sub>
Author(s)	Kato, Masaki; Ota, Ryo; Endo, Takashi et al.
Citation	ACS Applied Nano Materials, 5(2), 2367-2374 <a href="https://doi.org/10.1021/acsanm.1c04048">https://doi.org/10.1021/acsanm.1c04048</a>
Issue Date	2022-02-01
Doc URL	<a href="https://hdl.handle.net/2115/87812">https://hdl.handle.net/2115/87812</a>
Rights	This document is the Accepted Manuscript version of a Published Work that appeared in final form in ACS Applied Nano Materials, copyright © American Chemical Society after peer review and technical editing by the publisher. To access the final edited and published work see ACS Applied Nano Materials.
Type	journal article
File Information	20220117_SI_revise_no_mark.pdf



Supporting Information

# Free-standing Nanometer-Thick Covalent Organic Framework Films for Separating CO<sub>2</sub> and N<sub>2</sub>

*Masaki Kato<sup>1</sup>, Ryo Ota<sup>2</sup>, Takashi Endo<sup>2</sup>, Takashi Yanase<sup>3\*</sup>, Taro Nagahama<sup>1,4</sup>,*

*Toshihiro Shimada<sup>1,4\*</sup>*

<sup>1</sup> Graduate School of Chemical Science and Engineering, Hokkaido University, Kita 13 Nishi 8,  
Kita-ku, Sapporo 060-8628, Japan

<sup>2</sup> Center for Advanced Research of Energy and Material, Faculty of Engineering, Hokkaido  
University, Kita 13 Nishi 8, Kita-ku, Sapporo 060-8628, Japan.

<sup>3</sup> Department of Chemistry, Faculty of Science, Toho University, Miyama 2-2-1, Funabashi 274-  
8510, Japan

<sup>4</sup> Division of Applied Chemistry, Faculty of Engineering, , Hokkaido University, Kita 13 Nishi  
8, Kita-ku, Sapporo 060-8628, Japan

\*Corresponding authors:

[takashi.yanase@sci.toho-u.ac.jp](mailto:takashi.yanase@sci.toho-u.ac.jp) (T. Yanase), [shimadat@eng.hokudai.ac.jp](mailto:shimadat@eng.hokudai.ac.jp) (T. Shimada)

### **Definition and calculation of "ideal selectivity" and "separation factor"**

When the pure CO<sub>2</sub> or N<sub>2</sub> was permeated through the membrane, the permeance of each gas at each measurement point was calculated as follows (Eq. (1))

$$P = \frac{V}{A\Delta pRT} \left( \frac{dP}{dt} \right) \quad (1)$$

where  $V$  is the volume of the measurement room (15.3 cm<sup>3</sup>),  $A$  is the membrane area (1.33 cm<sup>2</sup>),  $\Delta p$  is the transmembrane pressure,  $R$  is the gas constant (8.31 J K<sup>-1</sup> mol<sup>-1</sup>),  $T$  is the absolute temperature (at the ambient condition) and  $dP/dt$  is the pressure increase per unit time in the measuring room.

The ideal selectivity of the pure gases was calculated as follows (Eq. (2))

$$\text{Ideal selectivity} = \frac{P_{\text{CO}_2}}{P_{\text{N}_2}} \quad (2)$$

where  $P_{\text{CO}_2}$  and  $P_{\text{N}_2}$  are the permeance of CO<sub>2</sub> and N<sub>2</sub>, respectively.

When the CO<sub>2</sub>-N<sub>2</sub> mixture was permeated through the membrane, the CO<sub>2</sub>/N<sub>2</sub> separation factor  $\alpha$  was calculated as follows (Eq. (3))

$$\alpha = \frac{y_{\text{CO}_2}/y_{\text{N}_2}}{x_{\text{CO}_2}/x_{\text{N}_2}} \quad (3)$$

where  $y_{\text{CO}_2}/y_{\text{N}_2}$  and  $x_{\text{CO}_2}/x_{\text{N}_2}$  are the ratios of the molar fraction in the permeate and feed sides, respectively.

### **Details of model analysis**

## 1 Gas permeation model of the COF films

The mechanism of gas sorption in a glassy polymer is explained by a dual site sorption model.<sup>1</sup>

In this model, the Henry sorption ( $C_D$ ) is the main mechanism of sorption into the matrix component, while Langmuir sorption ( $C_H$ ) governs the sorption into the microvoid region. The gas concentration in the polymer membrane ( $C$ ) is described as their sum

$$C = C_D + C_H = k_D p + \frac{C'_H b p}{1 + b p} \quad (4)$$

where  $k_D$  is Henry's law constant,  $p$  is the feed gas pressure,  $C'_H$  is the Langmuir capacity of the glassy polymer, and  $b$  is the Langmuir affinity constant.

The gas solubility coefficient ( $S$ ) is written as the following equation:

$$S = \frac{C}{p} = k_D + \frac{C'_H b}{1 + b p} \quad (5)$$

## 2 Partial immobilization model

When a gas diffuses in a polymer membrane, we consider both the Henry and Langmuir diffusion mechanisms.

It was assumed that the gas species, which are trapped in the Langmuir site, can be relatively mobile in the glassy polymer (partial immobilization).

We then estimated that the concentration of a gas in the polymer membrane is described by eq. (4), Fick's first law is eq. (6):

$$J = -D_D \frac{\partial C_D}{\partial x} - D_H \frac{\partial C_H}{\partial x} = -D_D \left( \frac{1 + \frac{FK}{(1+bp)^2}}{1 + \frac{K}{(1+bp)^2}} \right) \frac{\partial C}{\partial x} \quad (6)$$

where  $J$  is the flux of the gas species,  $D_D$  and  $D_H$  are the diffusion coefficient under the Henry and Langmuir modes, respectively,  $F$  is the ratio of  $D_D$  and  $D_H$  ( $D_D/D_H$ ), and  $K$  is equal to  $C'_H b/k_D$ .

By using eq. (6), Fick's second law is eq. (7):

$$\frac{\partial C}{\partial t} = \frac{\partial J}{\partial x} = \frac{\partial}{\partial x} \left( -D_D \left( \frac{1 + \frac{FK}{(1+bp)^2}}{1 + \frac{K}{(1+bp)^2}} \right) \frac{\partial C}{\partial x} \right) \quad (7)$$

Since the gas permeability ( $P$ ), gas diffusion coefficient ( $D$ ) and gas solubility coefficient ( $S$ ) of the polymer membrane have the relationship of  $P = DS$  (solution-diffusion mechanism), the average permeability ( $P_a$ ) of the membrane is eq. (8)

$$P_a = DS = -D_D \left( \frac{1 + \frac{FK}{1+bp}}{1 + \frac{K}{1+bp}} \right) S = k_D D_D \left( 1 + \frac{FK}{1+bp} \right) \quad (8)$$

### 3 Numerical analysis of gas permeation through the COF films

Generally, the dual mode sorption model parameters ( $C'_H$ ,  $b$ , and  $k_D$ ) can be obtained by using a non-linear curve fitting for the experimental gas sorption isotherms using eq. (4). However, the amount of gases absorbed in the COF film prepared by the alternating deposition cannot be experimentally measured

because its thickness is extremely thin. We determined the parameters by numerically solving eq. (7) by the finite differential method and adjusting its solution to the experimental permeation curve. An analysis program was built by the python 3.7.1 environment. Eq. (7) was numerically solved using the Crank-Nicolson method along with the Gauss-Seidel method. The appropriate parameters were calculated by minimizing the residual sum of squares of the numerical solution and experimental data. Algorithms for searching the minimum value used the differential-evolution method, which can search for the global minimum of a system.

#### 4 DFT calculation

The interaction energy between the COF and the gas molecules was calculated by the density functional theory (DFT). The calculations were performed using the Gaussian 16W package. To consider weak interactions between the atoms, the D3 dispersion correction reported by Grimme is included in the DFT calculations (DFT-D).<sup>2</sup> Basis sets of the 6-31 G (d)<sup>3</sup> and B3LYP<sup>4, 5</sup> functional were used for the structure optimization. The total energies of the optimized structures were calculated using the basis sets of the 6-311G(d) and B3LYP functional. The basis set superposition error was corrected using the counterpoise method.<sup>6</sup>

The interaction energies between the COF and the gas molecules( $\Delta E$ ) were calculated using the following equation (Eq.(4)).

$$\Delta E = E_{\text{COF+gas}} - (E_{\text{COF}} + E_{\text{gas}})$$

where  $E_{\text{COF}+\text{gas}}$  is the total energy of the COF with gas molecules at a binding site, and  $E_{\text{COF}}$  and  $E_{\text{gas}}$  are the energies of the COF and the gas molecules, respectively.

### **Reference in Supporting Information**

(1) Barrer, R. M. Diffusivities in Glassy Polymers for the Dual Mode Sorption Model. *J. Memb. Sci.* **1984**, *18* (C), 25–35. DOI: 10.1016/S0376-7388(00)85023-1.

(2) Grimme, S.; Antony, J.; Ehrlich, S.; Krieg, H. A Consistent and Accurate Ab Initio Parametrization of Density Functional Dispersion Correction (DFT-D) for the 94 Elements H-Pu. *J. Chem. Phys.* **2010**, *132* (15), 154104. DOI: 10.1063/1.3382344.

(3) Lee, C.; Yang, W.; Parr, R. G. Development of the Colic-Salvetti Correlation-Energy into a Functional of the Electron Density Formula. *Phys. Rev. B.* **1988**, *37* (2), 785–789. DOI: 10.1103/PhysRevB.37.785

(4) Becke, A. D. Density - Functional Thermochemistry . III . The Role of Exact Exchange. *J. Chern. Phys.* **1992**, *98* (7), 5648–5652. DOI: 10.1063/1.464913

(5) Boys, S. F.; Bernardi, F. The Calculation of Small Molecular Interactions by the Differences of Separate Total Energies. Some Procedures with Reduced Errors. *Mol. Phys.* **1970**, *19* (4), 553–566. DOI: 10.1080/00268977000101561.

(6) Simon, S.; Duran, M.; Dannenberg, J. J. How Does Basis Set Superposition Error Change the Potential Surfaces for Hydrogen-Bonded Dimers? *J. Chem. Phys.* **1996**, *105* (24), 11024–11031. DOI: 10.1063/1.472902.



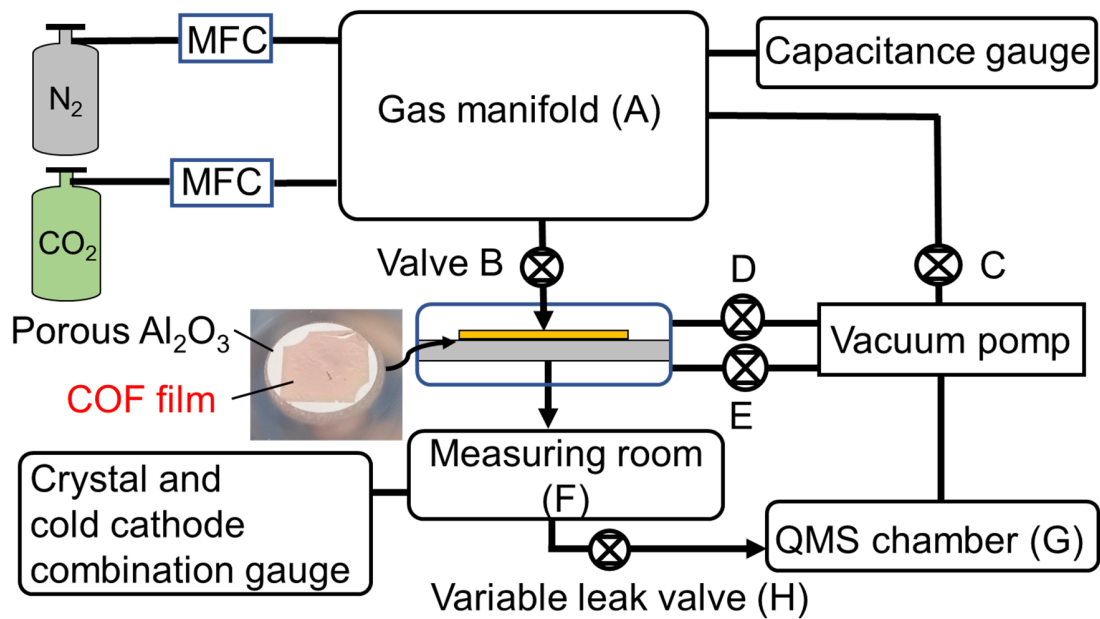


Figure S1. Schematic illustration of the apparatus for the gas permeation experiments.

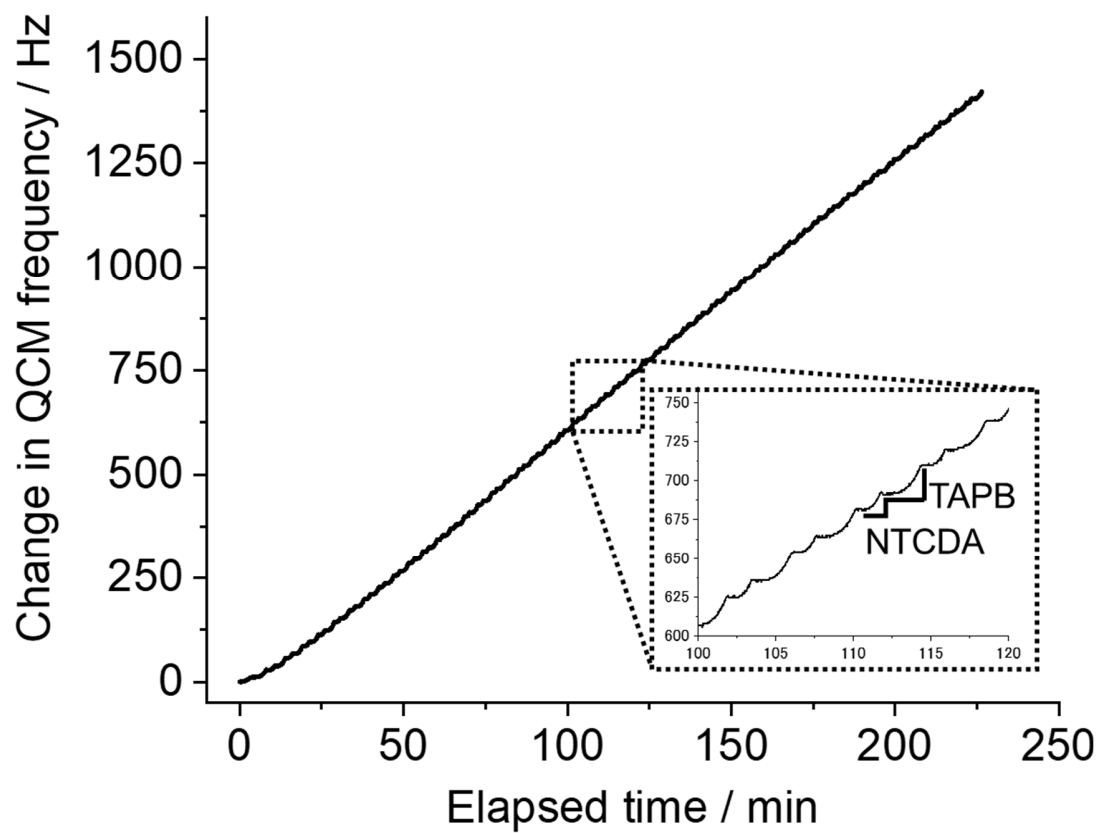


Figure S2: Decrease in the QCM frequency, which corresponds to the deposited amount of TAPB and NTCDA, occurred in a stepwise manner as shown in Fig. S2.

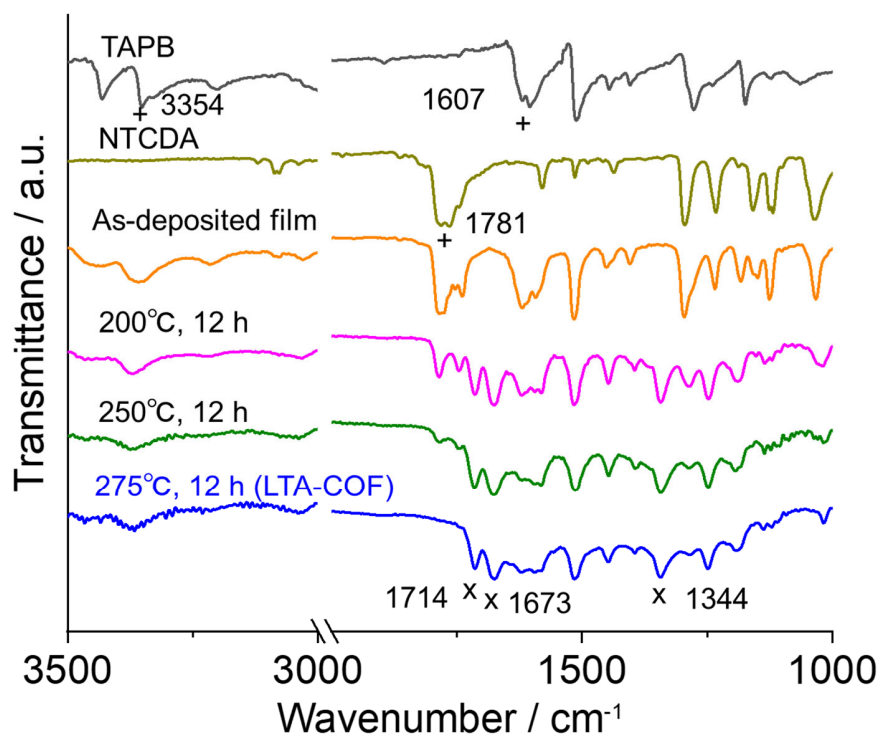


Figure S3: FTIR spectrum of precursors, as-deposited film (deposition ratio of TAPB : NTCDA = 1 : 2.5) and as-deposited film annealed at various temperatures for 12 h.

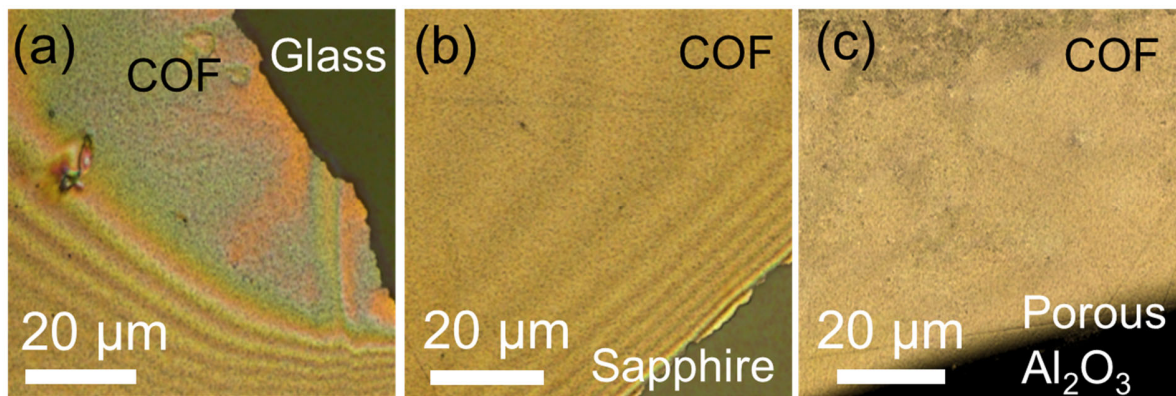


Figure S4: Laser microscope images of the film lifted out and transferred to different substrates from the water surface. Free-standing COF films placed on (a) a glass substrate, (b) a sapphire substrate, and (c) a porous Al<sub>2</sub>O<sub>3</sub> support.

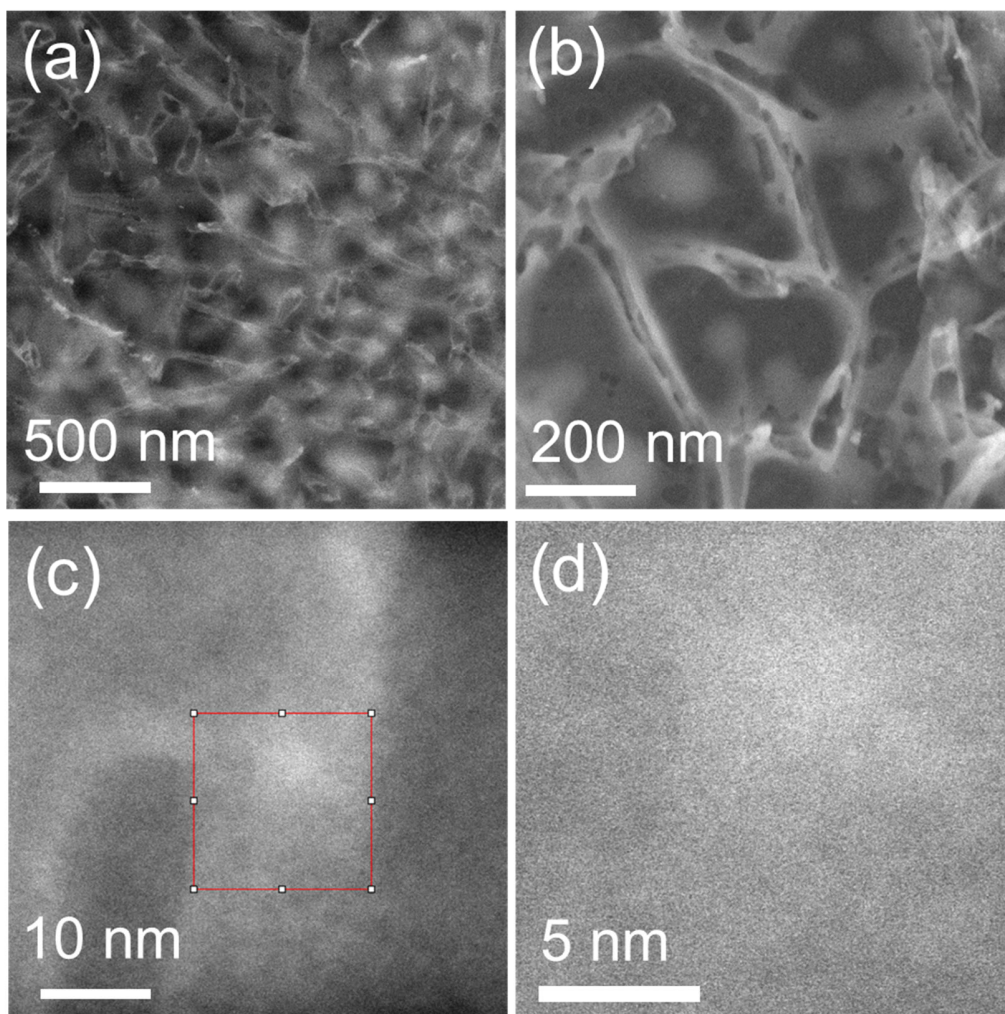


Figure S5: Examination of the LTA-COF film by STEM

(a), (b) Overall structure of the LTA-COF film

(c), (d) Further magnified images. (d) shows the red area of (c).

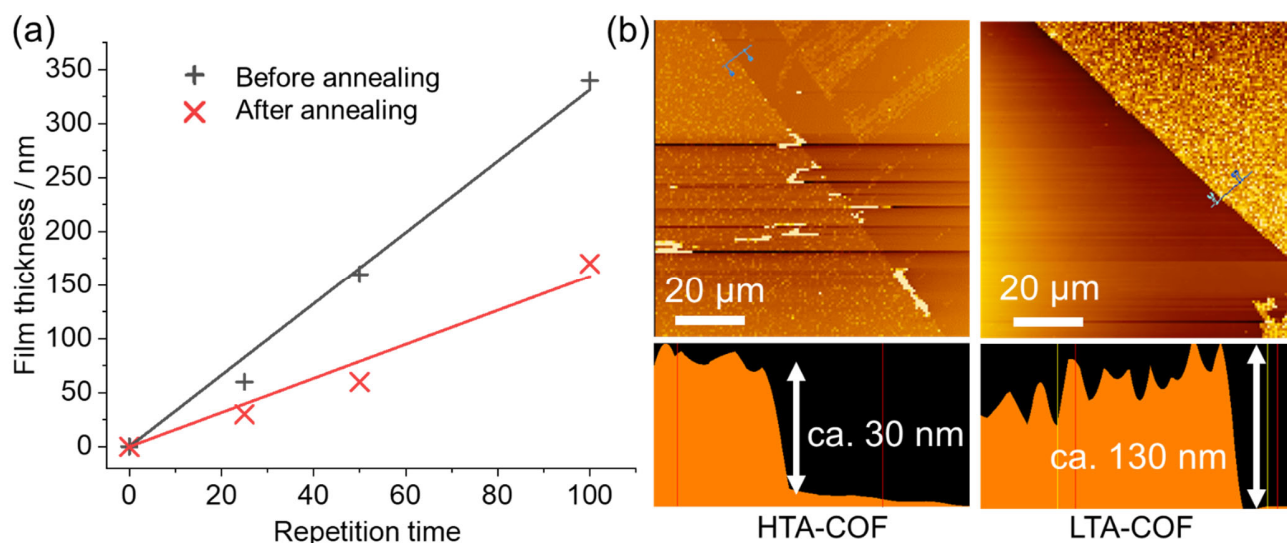


Figure S6: (a) The film thickness of the HTA-COF film for various repetition times (0-100). Black marks of “+” and red marks of “x” denote the film thickness of before and after annealing, respectively. The black and red lines are linear regression lines of each data set. (b) AFM measurement at the scraped edges of the HTA-COF and LTA-COF films (different repetition times) grown on SiO<sub>2</sub>/Si wafers.

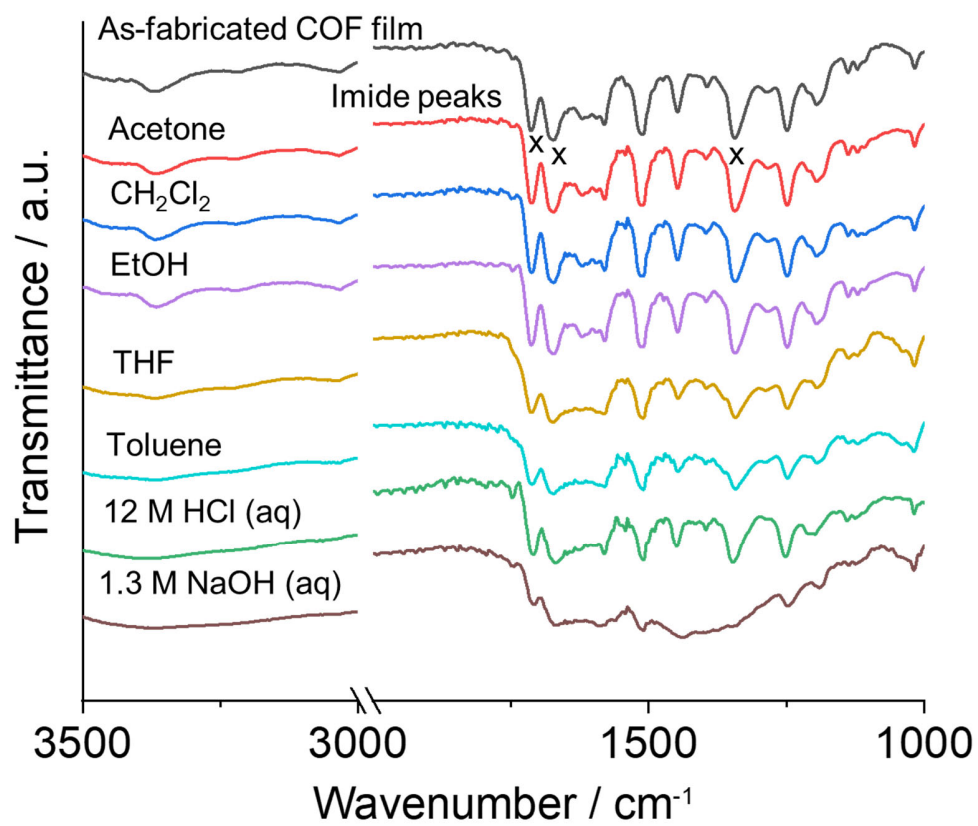


Figure S7: FTIR spectrum of the HTA-COF films before and after immersing in various solvents for 24 hours.

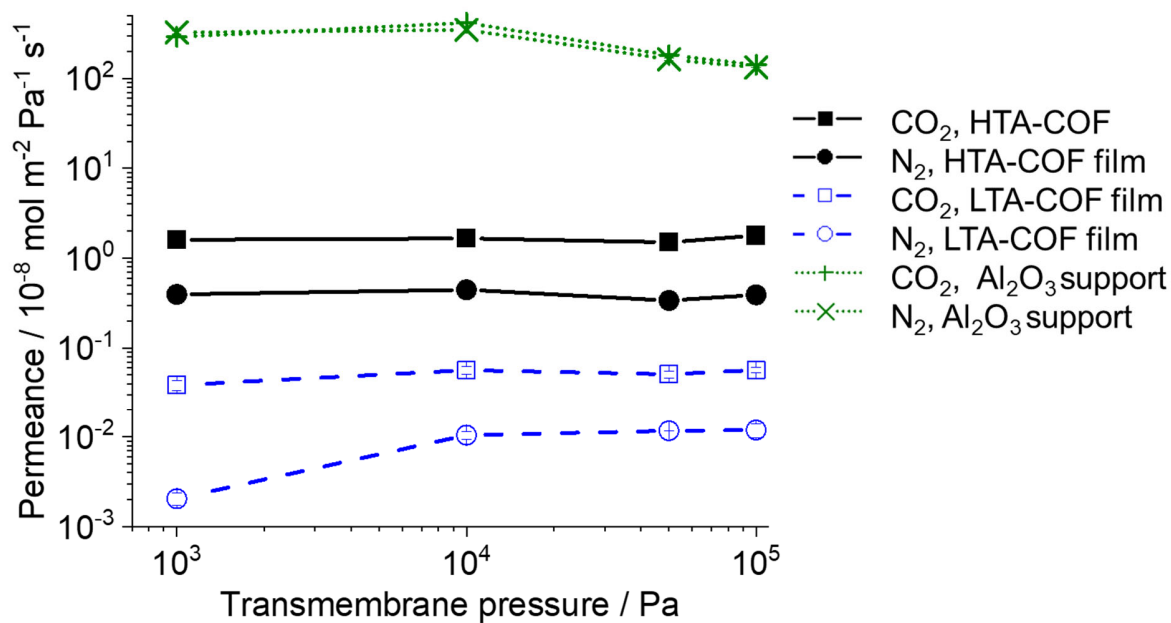


Figure S8: CO<sub>2</sub> and N<sub>2</sub> gas permeances of the HTA-COF films, LTA-COF films and a Al<sub>2</sub>O<sub>3</sub> support at the transmembrane pressures of 10<sup>3</sup>-10<sup>5</sup> Pa.

Note: CO<sub>2</sub> and N<sub>2</sub> permeances of the Al<sub>2</sub>O<sub>3</sub> support were sufficiently greater than that of the HTA- and LTA- COF film. These results indicated that the porous Al<sub>2</sub>O<sub>3</sub> support did not prevent CO<sub>2</sub> and N<sub>2</sub> from permeating through the membrane.

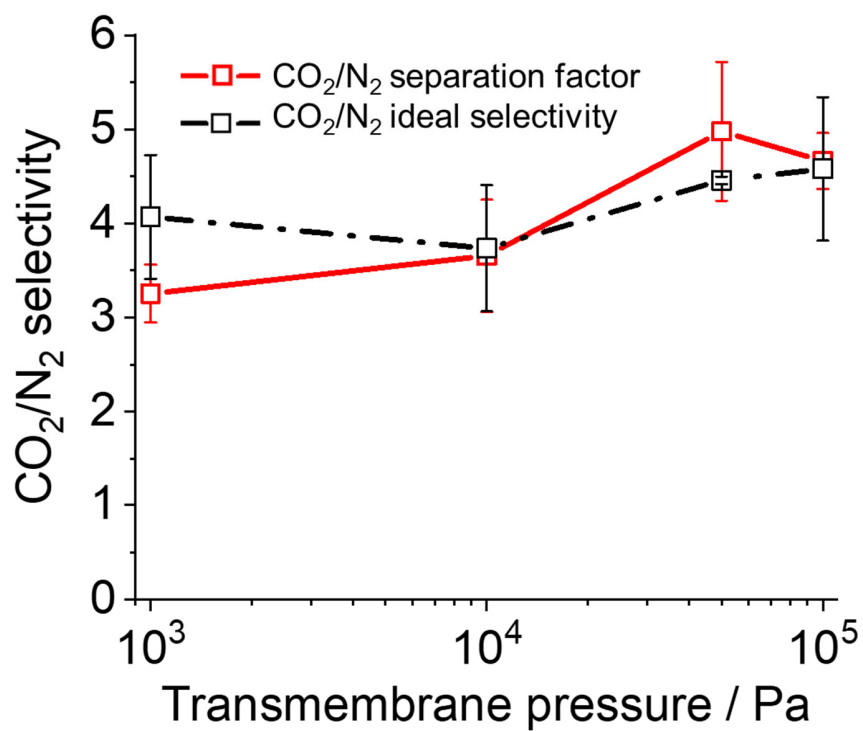


Figure S9: Pressure dependence of the CO<sub>2</sub>/N<sub>2</sub> separation factor and CO<sub>2</sub>/N<sub>2</sub> ideal selectivity for the HTA-COF film.